Multivariate pattern analysis links drug use severity to distributed cortical hypoactivity during emotional inhibitory control in opioid use disorder

Zhenhao Shi, PhD, Daniel D. Langleben, MD, Charles P. O'Brien, MD, PhD, Anna Rose Childress, PhD, Corinde E. Wiers, PhD

Center for Studies of Addiction, Department of Psychiatry, University of Pennsylvania Perelman School of Medicine, 3535 Market St Ste 500, Philadelphia, PA 19104

SUPPLEMENTARY INFORMATION

1. Mass-univariate analyses

Using a conventional mass-univariate approach, the individual "no-go vs. go" contrast images were subjected to (1) a one-sample t-test to identify brain regions showing an overall emotional inhibition effect, and (2) linear regression to identify an association between neural responses and drug use severity. Significant regions were determined using the threshold-free cluster-enhancement (TFCE) algorithm at cluster-level corrected $p<0.05$ (Smith and Nichols, 2009). The advantage of the TFCE algorithm is that it does not depend on an arbitrary cluster-forming threshold (i.e. voxel-level threshold) (Eklund et al., 2016) and is robust to the level of spatial smoothness (Smith and Nichols, 2009). We found that compared to go stimuli, no-go stimuli induced greater neural response in a number of regions listed in **Table S1** and shown in **Figure S1A**. No region showed significantly lower activity in response to no-go compared to go stimuli. We also found that drug use severity was negatively associated with neural response to no-go vs. go stimuli in the regions listed in **Table S2** and shown in **Figure S1B**. No region showed significantly positive association between drug use severity and neural response.

We additionally applied a threshold of voxel-level uncorrected $p<0.001$ combined with cluster-level $p<0.05$ corrected for familywise error (FWE) based on random field theory implemented in SPM 12. Regions showing greater neural response to no-go compared to go stimuli at this threshold are summarized in **Table S3**. No region showed greater neural response to go compared to no-go stimuli. Regions showing negative correlation between drug use severity and neural response to no-go vs. go stimuli revealed by regression analysis are summarized in **Table S4**. No region showed positive correlation with drug use severity.

We also applied a threshold of voxel-level FWE-corrected $p<0.05$. No region showed greater or weaker neural response to no-go compared to go stimuli at this threshold. Regions showing negative correlation between drug use severity and neural response to no-go vs. go stimuli revealed by regression analysis are summarized in **Table S5**. No region showed positive correlation with drug use severity.

2. Exploratory PLSR analysis on craving

We investigated the ability of brain activity to account for the individual differences in baseline and on-treatment opioid craving following the same PLSR analysis procedure described in the main article. We found that the cross-validated prediction error was significantly lower than those obtained from a 5000-iteration permutation test for on-treatment craving (observed MSE=6.62, 5th percentile of null MSE distribution=7.05, $p=0.030$) but only marginally so for baseline craving (observed MSE=6.20, 5th percentile of null MSE distribution=6.04, $p=0.063$). This is consistent with the finding that the PLSR score for drug use severity was more correlated with on-treatment craving than baseline craving, as reported in the main text. The optimal number of latent components across CV iterations was more variable for baseline craving (mean±SD=1.58±1.44, range=1–10) and on-treatment craving (1.12±0.56, range=1–4) than for drug use severity (1.02±0.20, range=1–3, see the main text). This may be due to subjective nature of craving and its susceptibility to several factors such as cognitive bias and memory inaccuracy (Sayette et al., 2000). Additional PLSR analysis on raw craving reduction (baseline minus on-treatment) and baseline-adjusted craving reduction did not show any significant association with neural response (raw, observed MSE=8.07, 5th percentile of null MSE distribution=6.14, $p=0.34$; baseline adjusted, observed MSE=6.30, 5th percentile of null MSE distribution=5.12, $p=0.25$).

3. Results from analyses that included the participant with excessive head motion

Consistent with the main analyses, drug use severity was associated with distributed brain hypoactivity in response to the no-go vs. go stimuli, as evidenced by significantly negative loadings in 879 of the 1000 cortical parcels (FDR-corrected p's<0.05). No regions showed significantly positive loadings. Of the 7 brain networks, the CCN and DAN had significantly more negative normalized engagement metrics compared to the average of other networks (CCN vs. others, –0.26 vs. –0.19, 95% bootstrap CI of difference=–0.11 to –0.02, FDR-corrected p=0.027; DAN vs. others, –0.27 vs. –0.19, 95% bootstrap CI of difference=–0.13 to –0.02, FDR-corrected p=0.030), while the LN engagement was significantly less negative than the average of other networks (–0.12 vs. –0.21, 95% bootstrap CI of difference=0.07 to 0.17, FDR-corrected p<0.001). The cross-validated prediction error was significantly lower than those obtained from a 5000-iteration permutation test (observed MSE=0.011, 5th percentile of null MSE distribution=0.011, p=0.046).

Drug use severity was significantly correlated with baseline opioid craving (r=0.43, p=0.027) but not on-treatment opioid craving (r=0.40, p=0.068). The PLSR brain score obtained from the multivariate neural response pattern was significantly correlated with both baseline opioid craving (r=0.46, p=0.018) and on-treatment opioid craving (r=0.62, p=0.002). Commonality analyses showed that the brain score and drug use severity made comparable unique contributions in accounting for the variance in baseline craving (ΔR^2=2.24%, 95% bootstrap CI=–22.20% to 22.61%, p=0.77). For on-treatment craving, the brain score made significantly greater unique contribution than drug use severity (ΔR^2=23.06%, 95% bootstrap CI=2.81% to 48.71%, p=0.023). Such greater contribution remained significant after on-treatment craving was adjusted for baseline craving (ΔR^2=16.23%, 95% bootstrap CI=0.53% to 43.91%, p=0.044).

4. References

Eklund, A., Nichols, T.E., Knutsson, H., 2016. Cluster failure: why fMRI inferences for spatial extent have inflated false-positive rates. Proceedings of the National Academy of Sciences of the United States of America 113, 7900-7905.

Sayette, M.A., Shiffman, S., Tiffany, S.T., Niaura, R.S., Martin, C.S., Shadel, W.G., 2000. The measurement of drug craving. Addiction 95, S189-S210.

Smith, S.M., Nichols, T.E., 2009. Threshold-free cluster enhancement: addressing problems of smoothing, threshold dependence and localisation in cluster inference. NeuroImage 44, 83-98.

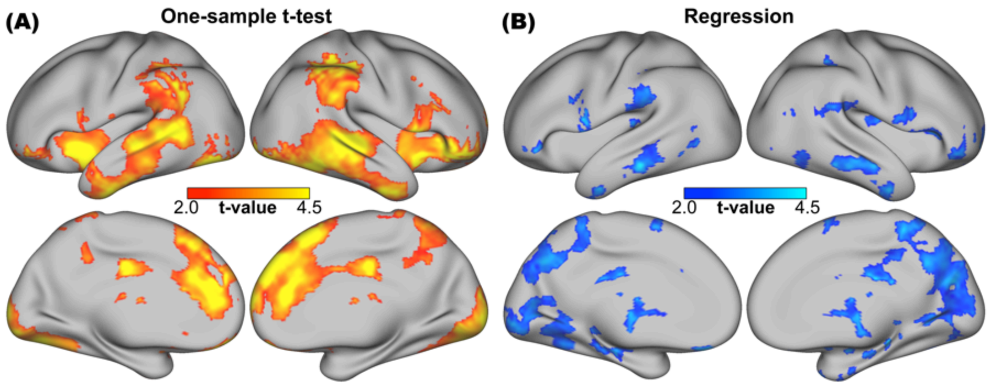

Figure S1. Results of mass-univariate analyses (thresholded at corrected p<0.05 using threshold-free cluster enhancement). **(A)** Regions showing greater neural response to no-go compared to go stimuli. **(B)** Regions showing negative correlation between drug use severity and neural response to no-go vs. go stimuli revealed by regression analysis.

Table S1. Regions showing greater neural response to no-go compared to go stimuli (threshold-free cluster enhancement)

Region	**Cluster extent**	**Z**	**MNI coordinates**
Left cerebellum	18272	5.66	–33/–85/–28
Anterior cingulate cortex		5.34	0/41/20
Right lingual gyrus		5.24	3/–82/–10
Left occipital pole		5.09	–6/–103/2
Right superior frontal gyrus		5.00	18/50/38
Right middle temporal gyrus		4.81	57/–43/–1
Right angular gyrus		4.75	45/–52/41
Right fusiform gyrus		4.59	33/–88/–22
Left middle temporal gyrus		4.53	–66/–43/–1
Right orbitofrontal gyrus		4.52	45/26/–19
Right cerebellum		4.51	30/–82/–31
Right occipital pole		4.50	18/–100/–1
Left inferior occipital gyrus		4.49	–33/–97/2
Supplementary motor area		4.47	0/2/71
Dorsomedial prefrontal cortex		4.47	–3/35/50
Left superior frontal gyrus		4.43	–18/53/26
Right inferior temporal gyrus		4.27	51/–7/–40
Right supramarginal gyrus		4.23	54/–34/56
Mid-cingulate cortex		4.21	0/–19/38
Left inferior temporal gyrus		4.20	–45/–25/–31
Right middle frontal gyrus		4.16	45/35/26
Right superior parietal lobule		4.13	42/–46/59
Right anterior insula		4.13	36/11/–13
Left orbitofrontal cortex		4.04	–21/53/–16
Left postcentral gyrus		3.74	0/–43/71
Right inferior frontal gyrus		3.74	57/20/5
Right temporal pole		3.62	57/14/–16
Left temporal pole		3.47	–45/5/–46
Left middle frontal gyrus		3.43	–36/59/2
Left superior parietal lobule		3.41	–45/–40/56
Right frontal pole		3.34	18/65/–1
Cerebellar vermis		3.34	–6/–64/–37
Left supramarginal gyrus		3.24	–51/–34/53
Right hippocampus		3.15	21/–19/–13
Precuneus		3.10	–6/–52/71
Right precentral gyrus		3.04	6/–25/74
Left inferior frontal gyrus		2.95	–57/17/17
Right posterior insula		2.95	36/–19/2
Left fusiform gyrus		2.84	–36/–22/–28
Left superior temporal gyrus		2.71	–60/–4/–4
Right superior temporal gyrus		2.61	63/–4/–4
Medial orbitofrontal gyrus		2.50	–6/29/–31
Left transverse temporal gyrus		2.37	–57/–16/8
Left frontal pole		2.36	–12/65/–13
Left entorhinal area		2.18	–15/5/–28
Left middle frontal gyrus	248	4.28	–39/14/44
Right entorhinal area	33	3.42	15/–1/–34
Right thalamus	108	2.96	6/–4/8
Left thalamus		2.65	–3/–16/14
Cerebellar vermis	27	2.69	3/–58/–4
Right cerebellum	30	2.62	6/–55/–22
Right cerebellum	11	2.35	6/–46/–61

Note: Significant regions identified at cluster-level $p<0.05$ using the threshold-free cluster-enhancement algorithm; cluster extent represents number of voxels with 3×3×3 mm^3 spatial resolution; MNI, Montreal Neurological Institute.

Table S2. Regions showing negative correlation between drug use severity and neural response (threshold-free cluster enhancement)

Region	Cluster extent	Z	MNI coordinates
Supplementary motor area	11347	4.60	3/2/71
Left fusiform gyrus		4.18	–39/–34/–25
Right fusiform gyrus		4.17	42/–34/–19
Right middle frontal gyrus		3.93	33/2/62
Precuneus		3.85	–3/–73/44
Left inferior temporal gyrus		3.77	–60/–31/–22
Cuneus		3.69	–6/–82/38
Right cerebellum		3.68	27/–34/–37
Left cerebellum		3.52	–24/–61/–31
Right middle temporal gyrus		3.47	51/–4/–34
Right superior parietal lobule		3.40	24/–40/62
Mid-cingulate cortex		3.28	3/–22/29
Cerebellar vermis		3.27	–6/–52/–19
Right middle occipital gyrus		3.22	45/–73/23
Right angular gyrus		3.21	36/–61/44
Right lingual gyrus		3.20	12/–67/–4
Right inferior frontal gyrus		3.10	51/17/11
Right supramarginal gyrus		3.06	39/–34/41
Left parahippocampal gyrus		3.05	–27/–22/–31
Posterior cingulate cortex		3.02	3/–31/26
Left lingual gyrus		3.02	–18/–61/–7
Right frontal pole		3.00	30/65/–7
Left superior parietal lobule		2.97	–9/–70/62
Right precentral gyrus		2.95	54/11/20
Left orbitofrontal gyrus		2.94	–24/8/–25
Right anterior insula		2.94	36/11/–10
Right inferior temporal gyrus		2.94	63/–37/–22
Right calcarine cortex		2.92	6/–88/5
Left supramarginal gyrus		2.90	–63/–31/26
Right inferior occipital gyrus		2.86	39/–85/–4
Right parahippocampal gyrus		2.83	21/–16/–34
Left calcarine cortex		2.81	–6/–82/5
Left transverse temporal gyrus		2.78	–51/–19/8
Right superior temporal gyrus		2.78	66/–40/20
Left central operculum		2.77	–63/–16/11
Right posterior insula		2.73	33/–19/14
Right temporal pole		2.71	39/11/–46
Right central operculum		2.70	51/–7/8
Right orbitofrontal cortex		2.65	42/53/–13
Left hippocampus		2.64	–21/–22/–10
Left inferior occipital gyrus		2.61	–54/–70/–7
Left occipital pole		2.51	–9/–100/–13
Right superior frontal gyrus		2.48	24/50/23
Left middle temporal gyrus		2.47	–66/–37/–10
Left superior occipital gyrus		2.41	–21/–85/26
Right postcentral gyrus		2.24	60/–13/32
Right hippocampus		2.23	27/–37/–1
Right parietal operculum		2.21	45/–22/17
Left postcentral gyrus		2.20	–24/–37/59
Left planum temporale		2.20	–51/–28/8
Right ventral tegmental area/substantia nigra	963	3.82	9/–10/–10
Left caudate		3.59	–9/17/5
Medial orbitofrontal gyrus		3.35	–12/47/–25
Right caudate		3.33	12/17/–1
Right thalamus		3.23	3/–4/11
Left orbitofrontal gyrus		3.20	–45/50/–10
Left middle frontal gyrus		3.14	–42/56/5
Right orbitofrontal gyrus		3.08	21/14/–28
Left middle frontal gyrus	73	3.57	–30/8/56
Left inferior temporal gyrus	91	3.30	–39/–1/–49
Left middle temporal gyrus		3.12	–51/–1/–40
Left thalamus	24	3.27	–3/–19/14
Right thalamus		2.82	6/–19/17
Left middle frontal gyrus	245	3.27	–48/8/47
Left inferior frontal gyrus		3.18	–60/11/14
Left cerebellum	38	3.22	–48/–49/–40
Left anterior insula	18	2.72	–39/2/2

Table S2. (Continued)

Anterior cingulate cortex	15	2.46	–9/26/29
Right cerebellum	12	2.36	18/–43/–58
Anterior cingulate cortex	25	2.28	12/26/32
Mid-cingulate cortex		2.14	6/17/26
Right cerebellum	10	2.24	39/–79/–40

Note: Significant regions identified at cluster-level $p<0.05$ using the threshold-free cluster-enhancement algorithm; cluster extent represents number of voxels with 3×3×3 mm^3 spatial resolution; MNI, Montreal Neurological Institute.

Table S3. Regions showing greater neural response to no-go compared to go stimuli (conventional cluster-level $p<0.05$)

Region	Cluster extent	Z	MNI coordinates
Left cerebellum	2886	5.66	–33/–85/–28
Right lingual gyrus		5.24	3/–82/–10
Left occipital pole		5.09	–6/–103/2
Right middle temporal gyrus		4.81	57/–43/–1
Right fusiform gyrus		4.59	33/–88/–22
Right cerebellum		4.51	30/–82/–31
Right occipital pole		4.50	18/–100/–1
Left inferior occipital cortex		4.49	–33/–97/2
Right inferior temporal gyrus		4.19	54/–34/–22
Left fusiform gyrus		3.89	–15/–97/–13
Left orbitofrontal cortex	262	5.59	–39/20/–19
Left inferior frontal gyrus		3.70	–51/35/–10
Anterior cingulate gyrus	1894	5.34	0/41/20
Right superior frontal gyrus		5.00	18/50/38
Right orbitofrontal gyrus		4.52	45/26/–19
Supplementary motor area		4.47	0/2/71
Dorsomedial prefrontal cortex		4.47	–3/35/50
Left superior frontal gyrus		4.43	–18/53/26
Right middle frontal gyrus		4.16	45/35/26
Right anterior insula		4.13	36/11/–13
Medial orbitofrontal cortex		4.04	15/53/–19
Right inferior frontal gyrus		3.74	57/20/5
Right temporal pole		3.62	57/14/–16
Right frontal pole		3.34	18/65/–1
Right angular gyrus	627	4.75	45/–52/41
Right supramarginal gyrus		4.23	54/–34/56
Right superior parietal lobule		4.13	42/–46/59
Left middle temporal gyrus	442	4.53	–66/–43/–1
Left inferior temporal gyrus		4.20	–45/–25/–31
Left temporal pole		3.47	–45/5/–46
Left orbitofrontal cortex	144	4.35	–36/53/–13
Medial orbitofrontal gyrus		4.12	–12/50/–25
Left middle frontal gyrus		3.43	–36/59/2
Left angular gyrus	234	4.08	–45/–52/32
Left superior parietal lobule		3.41	–45/–40/56
Left supramarginal gyrus		3.24	–51/–34/53
Right middle frontal gyrus	92	3.62	39/26/38

Note: Significant regions identified at voxel-level uncorrected $p<0.001$ combined with cluster-level $p<0.05$ corrected for familywise error based on random field theory; cluster extent represents number of voxels with 3×3×3 mm³ spatial resolution; MNI, Montreal Neurological Institute.

Table S4. Regions showing negative correlation between drug use severity and neural response (conventional cluster-level p<0.05)

Region	Cluster extent	Z	MNI coordinates
Right fusiform gyrus	103	4.17	42/–34/–19
Right middle temporal gyrus		3.47	51/–4/–34
Precuneus	93	3.85	–3/–73/44
Cuneus		3.69	–6/–82/38

Note: Significant regions identified at voxel-level uncorrected p<0.001 combined with cluster-level p<0.05 corrected for familywise error based on random field theory; cluster extent represents number of voxels with 3×3×3 mm³ spatial resolution; MNI, Montreal Neurological Institute.

Table S5. Regions showing negative correlation between drug use severity and neural response (conventional voxel-level p<0.05)

Region	Cluster extent	Z	MNI coordinates
Left cerebellum	57	5.66	–33/–85/–28
Left orbitofrontal cortex	46	5.59	–39/20/–19
Anterior cingulate cortex	15	5.34	0/41/20
Right lingual gyrus	24	5.24	3/–82/–10
Left occipital pole	6	5.09	–6/–103/2
Right superior frontal gyrus	8	5.00	18/50/38
Left cerebellum	5	4.93	–42/–58/–46
Right middle temporal gyrus	9	4.81	57/–43/–1
Right medial prefrontal gyrus	3	4.80	12/56/29
Right angular gyrus	4	4.75	45/–52/41
Supplementary motor area	2	4.68	6/26/56
Right lingual gyrus	4	4.64	15/–91/–19
Left occipital pole	1	4.62	–15/–103/5

Note: Significant regions identified at voxel-level p<0.05 corrected for familywise error; cluster extent represents number of voxels with 3×3×3 mm^3 spatial resolution; MNI, Montreal Neurological Institute.